Surface-tension-driven nanoelectromechanical relaxation oscillator

B. C. Regan,[a] S. Aloni,[b] K. Jensen,[c] and A. Zettl[d]
Department of Physics, University of California at Berkeley, and Materials Sciences Division, Lawrence Berkeley National Laboratory, Berkeley, California 94720

(Received 10 November 2004; accepted 2 February 2005; published online 18 March 2005)

Because of its linear dependence on length scale, surface tension can be a dominant force for small systems. Properly harnessed, this force is uniquely suited for nanomechanical applications. We have developed a nanoelectromechanical relaxation oscillator with a surface-tension-driven power stroke. The oscillator consists of two liquid metal droplets exchanging mass, and its frequency is directly controlled with a low-level dc electrical voltage. © *2005 American Institute of Physics*. [DOI: 10.1063/1.1887827]

The relative importance of different forces is scale dependent.[1] For instance, human beings cannot carry twenty times their own weight, nor walk on water. Yet insects having such abilities are well known.[2,3] The explanation lies in the relative scaling of mass, muscle strength, and surface tension with the length scale s. Thus, relative to weight ($\sim s^3$), muscle strength ($\sim s^2$) and surface tension ($\sim s$) are one thousand and one million times more effective, respectively, for insects than for humans because of the thousandfold difference in linear length scale. As the relevant size scale decreases, the relatively feeble scaling of surface tension makes it progressively more important. In the micrometer and nanometer regimes, this force can dominate.

Though often an impediment,[4–7] surface tension has been utilized in some synthetic microsystems. For instance, electric-field-induced changes in surface tension (electrowetting) are used to transport and manipulate droplets in microfluidic systems.[8,9] Microscale surface tension-based bubble valves and pumps have been developed for commercially available inkjet printers and lab-on-a-chip implementations.[10,11] A microelectromechanical systems (MEMS) technology[12] for three-dimensional assembly uses the surface tension forces created by melting precisely sized metal pads to rotate released structures off of the substrate plane. The degree to which surface tension is exploited by these approaches is limited, however. In the case of electrowetting, the surface tension effect is differential and thus requires high voltage to access relatively moderate forces. In the other cases, the surface tension action is inherently unidirectional.

A device that fully realizes surface tension's great advantages should be nanoscale, where surface tension is strongest relative to other forces, and involve a controllable, reciprocating mechanical action. In this letter, we describe the utilization of surface tension forces in a nanoelectromechanical relaxation oscillator. Relaxation oscillators, which relate to such diverse phenomena as heartbeats,[13] leaky faucets,[14] and earthquakes,[15] are generically characterized by two distinct time scales: A fast relaxation phase and a slow recovery phase. In our oscillator implementation, the fast relaxation is a hydrodynamic event driven by surface tension. The slow portion of the oscillator cycle is electrically driven and involves atom-by-atom transport.[16] By avoiding hydrodynamic transport during the slow half-cycle, direct confrontation between the electrical and surface tension forces is circumvented. Thus, this device accesses the full strength of the surface tension forces during relaxation, yet only requires low voltages for operation.

Figure 1 schematically depicts the relaxation oscillator mechanism. Two molten metal particles are located adjacent to one another on a carbon nanotube substrate. Driving electrical current through the substrate initiates an atomic mass transport process[16] along the nanotube, moving metal from

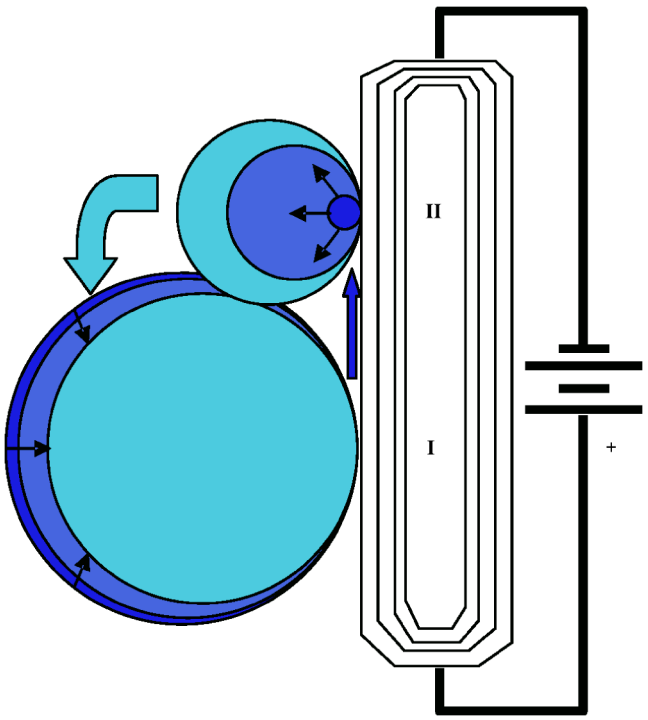

FIG. 1. (Color online). Schematic diagram of the nanoelectromechanical relaxation oscillator. Two liquid droplets are located at positions labelled I and II on a multiwalled carbon nanotube substrate. Driving an electrical current through the substrate induces atomic transport along the substrate from Droplet I to Droplet II (small arrow). The radius of the smaller droplet, II, increases more rapidly than the radius of the larger droplet, I, decreases, and eventually they touch. Surface tension forces then rapidly propel the mass at II back to position I through the newly created hydrodynamic channel. The repetition rate of the relaxation events, i.e., the oscillator frequency, is set by the magnitude of the dc electrical drive.

[a]Electronic mail: regan@physics.berkeley.edu
[b]Electronic mail: saloni@socrates.berkeley.edu
[c]Electronic mail: argon@socrates.berkeley.edu
[d]Electronic mail: azettl@socrates.berkeley.edu

the droplet at Site I to the one at Site II. This transport continues until Droplet II becomes large enough to touch the shrinking, but still larger, Droplet I. At that point, the fast phase of the relaxation oscillator cycle begins. Growing the smaller Droplet II at the larger Droplet I's expense is unfavorable from a surface energy standpoint.[17] The smaller droplet has a higher interfacial curvature and thus a higher internal pressure than the larger droplet. When a hydrodynamic channel is created by the physical contact of the two droplets, the pressure difference drives the fluid from the smaller droplet to the larger droplet, and the oscillator transitions from the metastable state. Droplet I consumes its offspring, and the process begins anew. The key advantage of using the process reported in Ref. 16 is that the recovery transport is atomic, not hydrodynamic. By moving atoms individually, via directed surface diffusion, the collective surface energy can be accumulated piecemeal, then rapidly released during the relaxation phase.

To observe its operation directly, we implement the device shown in Fig. 1 inside a JEOL 2010 transmission electron microscope (TEM). *Ex situ* indium metal is thermally evaporated onto a boule of arc-grown multiwall carbon nanotubes. Then, the nanotube sample is mounted on a piezodriven nanomanipulation stage and loaded into the microscope. Inside the microscope an individual nanotube or bundle is approached with the nanomanipulator, completing the electrical circuit indicated in Fig. 1. With suitably situated droplet nucleation sites, indium mass oscillation can be achieved and recorded with a charge coupled device video camera.

Figure 2(a) is a time series of TEM images showing relaxation oscillator operation. An applied voltage of 1.3 V drives 40 μA from bottom to top through the nanotube substrate. As many as four indium droplets are visible, depending on the frame. In these images, mass is leaving Droplet I, causing it to shrink, while the next Droplet II grows. Between Frames 3 and 4 Droplets I and II touch and the oscillator relaxes. While the gradual transport takes place over many seconds as dictated by the control voltage, the reset to the initial condition occurs rapidly compared to the video acquisition rate of 30 frames per second.

Figure 2(b) shows the control voltage as a function of time, and Fig. 2(c) gives the simultaneous masses of the two droplets. The masses have been calculated from the cross-sectional areas as determined by an automated image processing routine, assuming that the droplets are spheres $[\text{mass}=(7\ \text{g/cm}^3)(4\pi/3)(\text{area}/\pi)^{3/2}]$. Mass oscillations over many cycles are evident, with the small droplet showing slow growth followed by rapid relaxation. Although it is not immediately apparent in the still images, the automated analysis [Fig. 2(c)] shows that mass changes in the small droplet are anticorrelated with mass changes in the large, indicating excellent mass conservation within this two-droplet system. Changes in the control voltage lead to immediate changes in the mass transfer rate, and thus the oscillation frequency. TEM video showing this oscillator's operation is available; see EPAPS Ref. 18.

At constant control voltage, there are discernible ($\sim$0.6%) drops in the supplied current correlated with the relaxation of the oscillator of Fig. 2. The distribution of the metal on the nanotube substrate is thus affecting the resistance of the complete circuit, which bodes well for practical implementations of this oscillator. With the circuit resistance

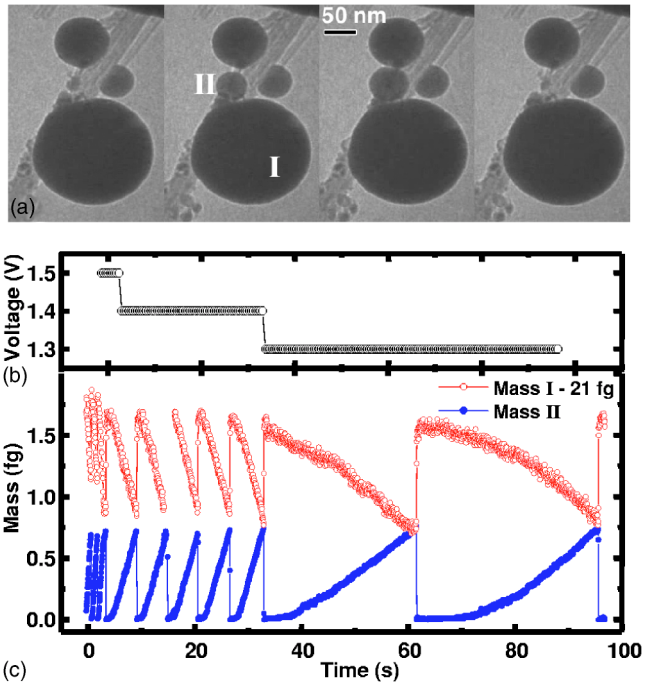

FIG. 2. (Color online). Implementation of the nanoelectromechanical relaxation oscillator. (a) A time series of four TEM video images showing one period of oscillator action. The second frame from the left shows the participating liquid indium droplets, labelled I and II as in the schematic Fig. 1. The suspended nanotube substrate, which is visible crossing the images diagonally, is carrying electrical current from the lower left to the upper right corners. In the first frame, the droplet at Position II is barely visible, but by the third frame it has grown to the point where it is nearly touching the droplet at Position I. In the fourth frame, the oscillator is seen directly after the subsequent relaxation event, when the mass distribution has been reset to a condition like that of the first frame. Parts (b) and (c) show the control voltage and the masses of the two participating droplets as a function of time, over many cycles with varying frequency. (Mass I has been offset by 21 fg for display purposes.) Although the time variation of Mass I is not obvious in the still images, the automated image processing routine reveals perfect anticorrelation with the more visually dramatic variation in Mass II. During the period shown, the drive voltage was adjusted from 1.5 to 1.3 V in two steps of 100 mV, with immediate changes resulting in the relaxation frequency.

as a built-in diagnostic of the oscillator phase, the additional complication and expense of an external monitor (in this case, the TEM) could become unnecessary in a well-characterized system. In an integrated device, electronics could conveniently monitor and, for instance, automatically adjust the oscillator frequency with closed-loop feedback.

The relaxation mechanism liberates appreciable energies in a very brief period. Immediately prior to a relaxation event, the small and large droplets of Fig. 2 have radii of about 30 and 90 nm, respectively. After relaxation, the large droplet's radius has increased to 91 nm. The surface tension γ of liquid indium at 400–500 °C is 0.54 N/m,[19] implying an energy release of 5 fJ per relaxation. In the viscous, small Reynolds number limit appropriate at these length scales, the time scale τ for the coalescence of the two droplets can be estimated[20] as $\tau \sim R\eta/\gamma$, where R is the characteristic drop radius and η is the metal viscosity (indium's viscosity is 1.3 mN s m^{-2} in the relevant temperature range).[21] This time scale, about 200 ps, implies that an oscillator based on this concept might operate at frequencies approaching the gigahertz range, subject of course to the time constraints of the slow phase. The speed of the relaxation event implies correspondingly large peak powers and forces: The oscillator

shown in Fig. 2 generates a peak power of $\sim 20\ \mu$W, and a peak force ~ 50 nN.

The most obvious applications of this nanoscale relaxation oscillator are locomotive,[22] as the oscillating metal droplets can exert substantial mechanical forces on neighboring objects. We have constructed numerous oscillators of similar design, including configurations where the growing and shrinking of the droplets causes the substrate nanotube to flex. Using device geometries demonstrated at the MEMS scale,[12] we imagine that efficient mechanical coupling to the oscillator could be arranged to provide large angular deflections. Such a nanoelectromechanical actuator promises a powerful combination of speed, simplicity, and strength, incorporating as it would high-frequency operation, low-voltage dc electrical drive, and surface tension's advantageous force scaling.

[1] W. S. N. Trimmer, Sens. Actuators **19**, 267 (1989).
[2] J. R. Adams, *Insect Potpourri: Adventures in entomology* (Sandhill Crane Press, Gainesville, Fla., 1992).
[3] D. L. Hu, B. Chan, and J. W. M. Bush, Nature (London) **424**, 663 (2003).
[4] T. F. Anderson, J. Appl. Phys. **21**, 724 (1950).
[5] C. H. Mastrangelo and C. H. Hsu, J. Microelectromech. Syst. **2**, 33 (1993).
[6] R. Maboudian and R. T. Howe, J. Vac. Sci. Technol. B **15**, 1 (1997).
[7] C. J. Kim, J. Y. Kim, and B. Sridharan, Sens. Actuators, A **64**, 17 (1998).
[8] J. Lee and C. J. Kim, J. Microelectromech. Syst. **9**, 171 (2000).
[9] S. K. Cho, H. J. Moon, and C. J. Kim, J. Microelectromech. Syst. **12**, 70 (2003).
[10] N. R. Tas, J. W. Berenschot, T. S. J. Lammerink, M. Elwenspoek, and A. van den Berg, Anal. Chem. **74**, 2224 (2002).
[11] F. G. Tseng, C. J. Kim, and C. M. Ho, J. Microelectromech. Syst. **11**, 427 (2002).
[12] R. R. A. Syms, E. M. Yeatman, V. M. Bright, and G. M. Whitesides, J. Microelectromech. Syst. **12**, 387 (2003).
[13] B. van der Pol and J. van der Mark, Philos. Mag. **6**, 763 (1928).
[14] A. Dinnocenzo and L. Renna, Phys. Rev. E **55**, 6776 (1997).
[15] M. V. Matthews, W. L. Ellsworth, and P. A. Reasenberg, Bull. Seismol. Soc. Am. **92**, 2233 (2002).
[16] B. C. Regan, S. Aloni, R. O. Ritchie, U. Dahmen, and A. Zettl, Nature (London) **428**, 924 (2004).
[17] A. W. Adamson and A. P. Gast, *Physical Chemistry of Surfaces*, 6th ed. (Wiley, New York, 1997).
[18] See EPAPS Document No. E-APPLAB-86-095512 for TEM video displaying a nanoelectromechanical relaxation oscillator's operation. A direct link to this document may be found in the online article's HTML reference section. The document may also be reached via the EPAPS homepage (http://www.aip.org/pubservs/epaps.html) or from ftp.aip.org in the directory /epaps/. See the EPAPS homepage for more information.
[19] M. A. McClelland and J. S. Sze, Surf. Sci. **330**, 313 (1995).
[20] J. Eggers, J. R. Lister, and H. A. Stone, J. Fluid Mech. **401**, 293 (1999).
[21] S. J. Cheng, X. F. Bian, J. X. Zhang, X. B. Qin, and Z. H. Wang, Mater. Lett. **57**, 4191 (2003).
[22] P. E. Kladitis and V. M. Bright, Sens. Actuators, A **80**, 132 (2000).